Available online at www.sciencedirect.com

Solid State Ionics 165 (2003) 257–267

SOLID STATE IONICS

www.elsevier.com/locate/ssi

An indium hexacyanoferrate–tungsten oxide electrochromic battery with a hybrid K^+/H^+-conducting polymer electrolyte

Tsai-Shih Tung, Lin-Chi Chen, Kuo-Chuan Ho*

Department of Chemical Engineering, National Taiwan University, Taipei 10617, Taiwan

Abstract

Electrochromic tungsten oxide (WO_3) and indium hexacyanoferrate (InHCF) thin-film electrodes, in combination with a polymer electrolyte that accommodates conduction of both K^+ and H^+, were assembled into a thin-film electrochromic battery (ECB). A typical InHCF–WO_3 ECB (designated as IWECB) can be charged and discharged reversibly between 0.5 and 1.5 V with a theoretical voltage of around 1.24 V. A hybrid K^+/H^+-conducting solid polymer electrolyte (SPE) was prepared through doping different amounts of KCl into poly-2-acrylamido-2-methylpropane sulfonic acid (PAMPS). The resultant SPE fulfilled the dual requirements: H^+ for the WO_3 and K^+ for the InHCF insertion/extraction. The KCl-doping level, evaluated from the molar ratio of (KCl)/(AMPS), plays a crucial role in determining the SPE properties, including its ionic conductivity and water content, and thus strongly affects the charge–discharge characteristics of the IWECB. Furthermore, both properties of the SPE exhibited a very similar, concave-up dependence on the doping level, and a minimum existed at (KCl)/(AMPS) = 0.44. It was found that the SPE with a higher KCl-doping level could achieve a larger discharge capacity and a higher cell voltage, but would result in a poorer cycle life. Although the charge capacity of the IWECB was limited, it is enough to drive many low-watt electronic devices for several hours. Finally, the capability of the IWECB was also demonstrated by storing solar energy and by visualizing the state-of-charge (SOC), in which a highly contrasting blue-to-colorless electrochromism in response to discharging was visualized.

PACS: 78.20.Jq; 42.79.We

Keywords: Electrochromic battery (ECB); Indium hexacyanoferrate (InHCF); Poly-2-acrylamido-2-methylpropane sulfonic acid (PAMPS); Solid polymer electrolyte (SPE); Tungsten oxide (WO_3)

1. Introduction

The electrochromic (EC) [1] material describes an electroactive species that changes color in response to a change in its redox state. With this unique property, EC materials have been investigated for many applications such as displays [2,3], antiglare mirrors [4], solar-attenuated windows [5], and secondary batteries [6–15]. Among the applications, thin-film secondary batteries based on EC electrodes are relatively new. A secondary thin-film EC battery (ECB) can be assembled from two EC thin-film electrodes which sandwich an electrolyte, so an ECB has a cell configuration essentially identical to that of a complementary EC device (ECD). Similar to an ECD, an ECB also exhibits different colors when the cell voltage changes. Consequently, ECBs can be used to judge the residual

---

* Corresponding author. Tel.: +886-2-2366-0739; fax: +886-2-2362-3040.

E-mail address: kcho@.ntu.edu.tw (K.-C. Ho).

0167-2738/$ - see front matter © 2003 Elsevier B.V. All rights reserved.
doi:10.1016/j.ssi.2003.08.057

capacity with the naked eye and thus increase the convenience of using a secondary battery.

Concerning the evolution of ECBs, Prussian blue (PB) is a very pivotal material. Table 1 summarizes the relevant ECB systems reported in literature. Based upon the high electrochemical reversibility in a K^+-containing electrolyte and the multiple redox states of Prussian blue (PB) (Berlin green (BG)↔PB↔Everitt's salt (ES)) [16,17], Neff [6] first reported a PB-based secondary battery employing an aqueous electrolyte. The battery, assembled of two identical PB/graphite electrodes, had a theoretical voltage of 0.68 V and a theoretical energy density of 95 mW h/cm^3. Next, Honda et al. [7,8] modified the Neff cell by using PB-coated ITO electrodes and Nafion® solid polymer electrolyte (SPE). They reported that the SPE considerably improved the cycle life of the cell. Recently, Jayalakshmi and Scholz [9] reported a large-capacity cell composed of PB/graphite paste electrodes and Nafion® SPE. Other relevant systems including Cu–PB cells [10,11], Prussian blue analogue (PBA)–PB cells [12,13], and WO_3–PB cells [14] have also been reported. However, among the above systems, only the Honda cell [7,8] and WO_3–PB cell [14] used transparent conductive substrates to exhibit the electrochromism of PB. Furthermore, all of the above PB-based batteries have a low discharge voltage except the WO_3–PB cell [14]. Thus, achieving a high visual contrast and a workable cell voltage is the crucial issue for fabricating ECBs.

In a recent work [15], we fabricated a new thin-film ECB based on indium hexacyanoferrate (InHCF) and tungsten oxide (WO_3), namely IWECB, and demonstrated its feasibility. The IWECB employed the KCl-saturated poly-2-acrylamido-2-methylpropane sulfonic acid (KCl-saturated PAMPS) SPE [18,19] to accommodate the conduction of both H^+ and K^+ ions. In comparison with ECB systems reported in literature, our IWECB showed a larger half discharge voltage and exhibited an obvious color change. The EC mechanisms for InHCF and WO_3 have been proposed in the literature [20–27] and are summarized as follows:

$$\begin{aligned}&\mathrm{In[Fe(CN)_6](yellowish)} + \mathrm{K}^+ + \mathrm{e}^- \\ &\quad \leftrightarrow \mathrm{KIn[Fe(CN)_6](colorless)}\end{aligned} \tag{1}$$

$$\mathrm{WO_3(colorless)} + x\mathrm{H}^+ + x\mathrm{e}^- \leftrightarrow \mathrm{H}_x\mathrm{WO_3(blue)} \tag{2}$$

The above EC switching behaviors can be clearly observed when reducing or oxidizing the EC films deposited on F-doped SnO_2 (FTO) glass substrates. We found that the formal potentials were 0.874 and −0.365 V (vs. Ag/AgCl/in the KCl-saturated PAMPS) for the InHCF/KInHCF and WO_3/H_xWO_3

Table 1
A partial list of the non-lithium ECB systems reported in literature

Cell configuration	Half discharge voltage (V)	Practical capacity or energy density	References
Graphite/PB^a/K_2SO_4/PB^b/Graphite	0.68	95 mW h/cm^3	[6]
ITO/PB^a/Nafion®/PB^b/ITO	0.68	50 W h/kg	[7,8]
PB_m/Nafion®/PB_m^{c}	ca. 1.0^d	20 A h/kg	[9]
Cu,X/X/PB,Graphite,X^e	0.38–0.47	28 mA h	[10,11]
Pt/CuHCF/K_2SO_4/PB/Pt	0.5	50 W h/kg	[12]
$ZnHCF_m$/Nafion®/PB_m^{f}	0.6–0.8	12 A h/kg	[13]
$CuHCF_m$/Nafion®/PB_m^{g}	0.87	5 A h/kg	[13]
FTO/PB^a/K-PAMPS^h/WO_3/FTO	1.30	37.8 mW s/cm^2	[14]
FTO/InHCF/K-PAMPS^h/WO_3/FTO	1.15	20.6 mW s/cm^2	[15]

[a] BG/PB redox couple.
[b] PB/ES redox couple.
[c] PB_m = a mixture of PB, graphite, KCl, HCl, and binders.
[d] The cell used the Prussian Yellow (PY)/PB and PB/ES redox couples.
[e] X = an electrolyte of copper ion, $Rb_4Cu_{16}I_{7-x}Cl_{13+x}$.
[f] $ZnHCF_m$ = a mixture of zinc hexacyanoferrate (ZnHCF), graphite, KCl, HCl, and binders.
[g] $CuHCF_m$ = a mixture of copper hexacyanoferrate (CuHCF), graphite, KCl, HCl, and binders.
[h] K-PAMPS = KCl-saturated poly-AMPS®.

redox couples, respectively. A maximum H^+ insertion level of around 0.33 in H_xWO_3 [14] was attained when a potential of -0.5 V (vs. Ag/AgCl/sat't KCl) was applied to the WO_3 electrode. Accordingly, an IWECB using the KCl-saturated PAMPS SPE has a theoretical voltage of around 1.24 V. The overall cell reaction is written as follows:

$$\underset{\text{(The fully discharged state)}}{3WO_3(\text{colorless}) + \text{KInHCF}(\text{colorless}) + H^+} \rightleftharpoons \underset{\text{(The fully charged state)}}{3H_{1/3}WO_3(\text{blue}) + \text{InHCF}(\text{yellowish}) + K^+} \quad (3)$$

Eq. (3) suggests that an IWECB exhibits reversible, colorless-to-blue electrochromism in response to a charging process. Eq. (3) also implies that the battery is in perfect balance, which would be very difficult to achieve in practice. Moreover, Eq. (3) elucidates that the cell requires both H^+ and K^+ for reversible operation.

In principle, InHCF prefers K^+ for its EC reaction, whereas WO_3 prefers protons [20–27]. Therefore, finding a suitable, mixed electrolyte of K^+ and H^+ became very crucial. Since poly-2-acrylamido-2-methylpropane sulfonic acid (PAMPS) itself had been proven to be a good proton conductor for ECDs [28–31], we considered that doping potassium ions into the sulfonic PAMPS matrix could also result in conduction of K^+. Thus, KCl-saturated PAMPS SPE was used in our first attempt for an IWECB and proved to be workable. In addition, such a KCl-saturated PAMPS SPE has been successfully applied to a PB–WO_3 ECB [14] and a PB–InHCF ECD [32]. Despite the successful introduction of SPE, the amount of KCl required for doping the PAMPS matrix in order to obtain optimal IWECB performance has not yet been discussed. Therefore, this work not only further demonstrates the viability of IWECB but also aims to determine the influences of the K^+-doping level in the KCl-doped PAMPS SPE on the EC electrodes and the resultant ECB. In this paper, the mechanism of dual ionic conduction of H^+ and K^+ in the SPE is discussed, as well as how the PAMPS SPEs with different KCl-doping levels affect the electrochemical behavior of the InHCF and WO_3 electrodes. Finally, the charge/discharge behavior and the cycle life of IWECB, as affected by the KCl-doping level, are illustrated and explained.

2. Experimental

All chemicals used in this work were reagent grade and were used as received. Deionized water (DIW) was used throughout this work. All experiments were carried out at room temperature. The experimental methods are described as follows.

2.1. Substrate

Optically transparent FTO glass substrates ($R_{sh} = 20$ Ω/sq., $T_{550\ nm} = 80\%$, Sinonar, Hsinchu, Taiwan) were used for the deposition of EC films. Before deposition, a FTO substrate with dimensions of 4.0 × 3.0 × 0.2 cm^3 was ultrasonically cleaned with 0.1 N HCl for 3 min and then rinsed with DIW. Afterwards, a piece of Cu tape (3M, 3.0 × 0.5 cm^2) was applied to one side of the FTO-coated surface as the bus bar, and then insulating tapes were applied to maintain an electrode area of 2.0 × 2.0 cm^2.

2.2. Preparation of the electrochromic electrodes

InHCF films were electrodeposited onto clean FTO glass substrates through the cyclic voltammetric (CV) method. The plating solution was composed of 10 mM $InCl_{3(aq)}$, 10 mM $K_3Fe(CN)_{6(aq)}$, 1 N KCl, and 1 N HCl. The excess potassium ions and protons were proven to considerably stabilize the InHCF plating solution [33]. During CV deposition, a dynamic potential, applied to a FTO substrate, was scanned repeatedly 40 times between 0.1 and 1.2 V (vs. Ag/AgCl/Sat'd KCl) at a rate of 0.2 V/s. The as-prepared InHCF films were washed with DIW and then dried in air for at least 24 h before using.

The WO_3 films were deposited potentiostatically onto FTO glass substrates. The deposition solution was composed of a 36.7 vol.% peroxy-tungsten acid (PTA) solution, 30.3 vol.% DIW, and 33.0 vol.% isopropanol. The PTA solution was prepared by dissolving 1.5 g tungsten powder into a mixture of 30 ml H_2O_2 (30%) and 30 ml DIW, which was modified from the references [34–36]. Since the dissolution process was highly exothermic, it was initially carried out in an ice bath. After the exothermic reaction became milder, the solution was placed in air at room temperature for 24 h to complete the dissolution. Then a platinum-black coated Pt foil was immersed into the PTA solution for another 20 h to decompose the excess H_2O_2. Finally, the filtrated PTA solution was used. During WO_3 deposition, a constant potential of -0.45 V (vs. Ag/AgCl/Sat'd KCl) was applied to the FTO substrate until 1.0 C was passed (~ 22 min). The as-grown WO_3 films were washed with DIW and then fired at 100 °C for 1 h to attain good EC reversibility [34].

2.3. Preparation of monomer solutions and solid polymer electrolytes

An undoped AMPS monomer solution composed of 47.61 wt.% 2-acrylamido-2-methylpropane sulfonic acid (AMPS), 50.65 wt.% DIW, 1.69 wt.% tetra-(ethylene glycol) diacrylate (TEGDA), and 0.05 wt.% bezoin methyl ether (BME) was first prepared. AMPS, DIW, TEGDA, and BME are the monomer, solvent, cross-linking agent, and initiator, respectively. Then, five AMPS monomer solutions (denoted by solutions a–e) added with different amounts of KCl were prepared resulting in five PAMPS SPEs with different K^+-doping levels. The molar ratios of KCl to AMPS ((KCl)/(AMPS)) are 2.18×10^{-3}, 2.18×10^{-2}, 2.18×10^{-1}, 4.36×10^{-1}, and 5.41×10^{-1} for the above solutions, respectively. The pH and pK values of the above solutions were measured using commercial pH and pK meters (ORION, 91-72 BN and 9700 BN), respectively.

Polymerization was carried out in a casting mold ($2.0 \times 2.0 \times 0.2$ cm^3), and they were cured by a 3-min exposure to UV irradiation (Spectroline, SB-125, 675 μW/cm^2) [30]. In addition to the KCl-doped PAMPS electrolyte, pure undoped PAMPS SPE was also prepared for comparison. The ionic conductivity of each SPE was measured with impedance spectroscopy (ECO-Chemie, Autolab, PGSTAT30). During the measurement, a piece of SPE thick film (about 1.2 mm in thickness) was clipped in between the two platinum plates with an electrode area of 1.0×1.0 cm^2. The water content of each SPE was determined by measuring the weight loss after drying in an oven at 90 °C for 18 h [18].

2.4. Assembly of electrochromic batteries

For the assembly of an IWECB, an as-prepared InHCF electrode and a post-heated WO_3 electrode were used as the positive and negative electrodes, respectively. A fresh SPE film was sandwiched in between the face-to-face EC electrodes in the presence of a 2-mm-thick spongy-rubber spacer. The laminated IWECB was tightly clipped and was then ready for further characterizations. Assembly was carried out in ambient conditions at room temperature, and neither electrode was prepolarized. In addition, to study the effects of the K^+-doping level in SPE, IWECBs were fabricated using all of the above-mentioned SPEs.

2.5. Electrochemical and optical measurements for electrodes and batteries

The InHCF and WO_3 electrodes were characterized electrochemically in the presence of different KCl-doped PAMPS SPEs. Using the three-electrode CV method, the formal potentials and redox capacities of the InHCF/KInHCF and WO_3/H_xWO_3 redox systems were estimated. The voltammetry was performed using a potentiostat/galvanostat (ECO-Chemie, Autolab, PGSTAT30); silver wire and a platinum plate were used as the pseudo-reference and auxiliary electrodes, respectively.

IWECBs were characterized by two-electrode chronopotentiometry with a multi-channel battery test system (Maccor, Model 2300). When characterizing an IWECB, the cell voltage (InHCF vs. WO_3) was recorded. In addition, an in situ spectroelectrochemical method was employed to characterize the electrochromism of the IWECBs. The ECB was connected to the potentiostat/galvanostat and placed in a spectrophotometer (Shimadzu, model UV-1601PC) to collect the transmittance spectra at different equilibrated cell voltages. In addition, a commercial 8-digit electronic calculator (CASIO, LC-403LD) and a photovoltaic cell (Sinonar, SC-5030, 1.8 V/26 mA at 100 mW/cm^2) were used to demonstrate the applicability of the IWECB.

3. Results and discussions

3.1. Electrochemical and optical performances of the IWECB using the KCl-saturated PAMPS SPE

3.1.1. Typical charge/discharge characteristics and electrochromism

It was demonstrated in our previous work that an IWECB could be reversibly charged/discharged when

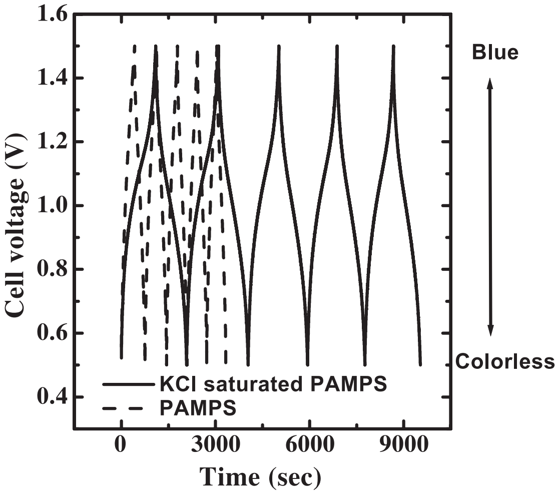

Fig. 1. Typical charge–discharge curves (voltage–time plot) of two different IWECBs. Solid line: charge–discharge curve for the IWECB using the KCl-sat'd PAMPS SPE ((KCl)/(AMPS) = 0.54). The individual charge capacities for InHCF and WO_3 were calculated from CVs (see Figs. 7e and 8e) and were 29 and 40 mC/cm^2, respectively. Dashed line: charge–discharge curve for the IWECB using the unmodified PAMPS SPE. Charge–discharge rate is 0.025 mA/cm^2.

using the KCl-saturated PAMPS SPE [15]. This fact implies that such an SPE really accommodates the conduction of K^+. To further verify this argument, Fig. 1 compares the charge/discharge curves of two different IWECBs using KCl-saturated PAMPS and unmodified PAMPS SPEs, respectively. It can be seen that the IWECB with the KCl-saturated SPE provided a capacity of around three times larger than that of the cell employing the unmodified SPE. This means that a KCl-saturated PAMPS is superior to PAMPS for an IWECB due to accommodating both K^+ and H^+ ions. The effects of KCl doping in PAMPS are presented and thoroughly discussed in the following subsections. In addition, Fig. 1 shows that the IWECB with the KCl-saturated PAMPS SPE can be reversibly charged/discharged between 0.5 and 1.5 V at a rate of 0.025 mA/cm^2 and exhibits a discharge capacity of around 26.0 mC/cm^2. This discharge capacity was calculated from Fig. 1 according to $q = it$. Although the thin-film IWECB provides a relatively small capacity, it still can serve as a power source for low-watt electronic devices, as discussed in Section 3.1.2.

Apart from the charge–discharge characteristics which are identical to that of a typical secondary battery, the IWECB also exhibits vivid blue-to-colorless electrochromism when discharging [15]. Therefore, such a high visual contrast between the charged and discharged states realizes the visualization of state-of-charge (SOC). In a practical sense, the SOC can only be judged by the naked eye as the device changes color continuously. With the help of a spectrophotometer, one can obtain the value quantitatively [14]. To understand if the electrochromism can be used as a warning sign for recharging the battery, the cell voltage at which the change in transmittance is most obvious must be determined. Since the blue-to-colorless electrochromism is attributed to additive EC behaviors of InHCF (yellowish/colorless) and WO_3 (blue/colorless), Fig. 2 plots the differential transmittances (dT/dV) of an IWECB at 410 nm (characteristic wavelength for InHCF) and 650 nm (characteristic wavelength for WO_3) as a function of cell voltage (V). The differential transmittances are calculated from an equilibrated $T-V$ curve [15]. It is shown in Fig. 2 that the maximum dT/dV values for 410 and 650 nm exist at around 1.05 and 0.92 V, respectively. In addition, the maximum dT/dV value at 650 nm is larger than that at 410 nm. These facts indicate that the most obvious blue-to-colorless color change occurs when the cell voltage passes

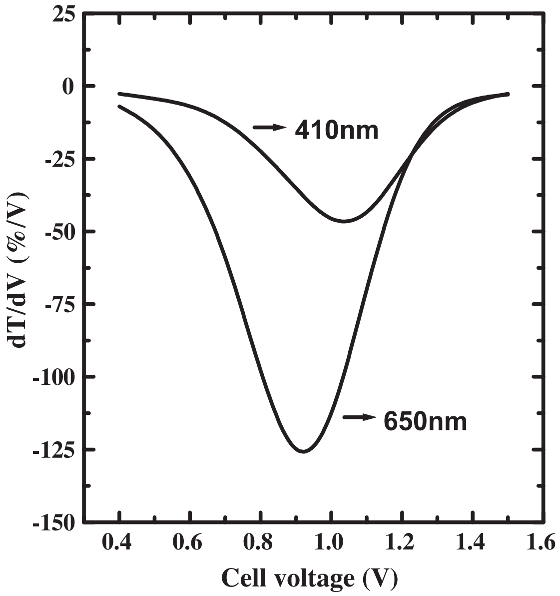

Fig. 2. Differential transmittances (dT/dV) at 410 and 650 nm of an IWECB using the KCl-sat'd PAMPS SPE as functions of the cell voltage.

through around 0.92 V. Since many low-watt electronic devices cannot function normally with a power source production of smaller than 0.9 V, the highest visual contrast at 0.92 V of the IWECB will be applicable for low-watt electronic devices.

3.1.2. Multiple energy-saving functions of the IWECB

The energy capacity of around 26.0 mW s/cm^2 and the blue-to-colorless electrochromism not only assure that an IWECB can act as a rechargeable battery, but also that it can meet applications to solar attenuation and the storage of solar energy. By serving as a rechargeable battery, an IWECB can drive a low-power electronic device (e.g., electronic timer, electronic temperature and/or humidity indicator, and electronic calculator) for a few hours [14]. As for its application as an EC window, Spindler [31] documented an InHCF–WO_3 EC system similar to our IWECB. The application for storing solar energy is demonstrated in Fig. 3. This figure shows that a photovoltaic (PV) cell connected to an IWECB can function as an all-solar-driven electronic calculator, in which the IWECB stores the solar energy collected by the PV cell and then drives the calculator. By considering all of the

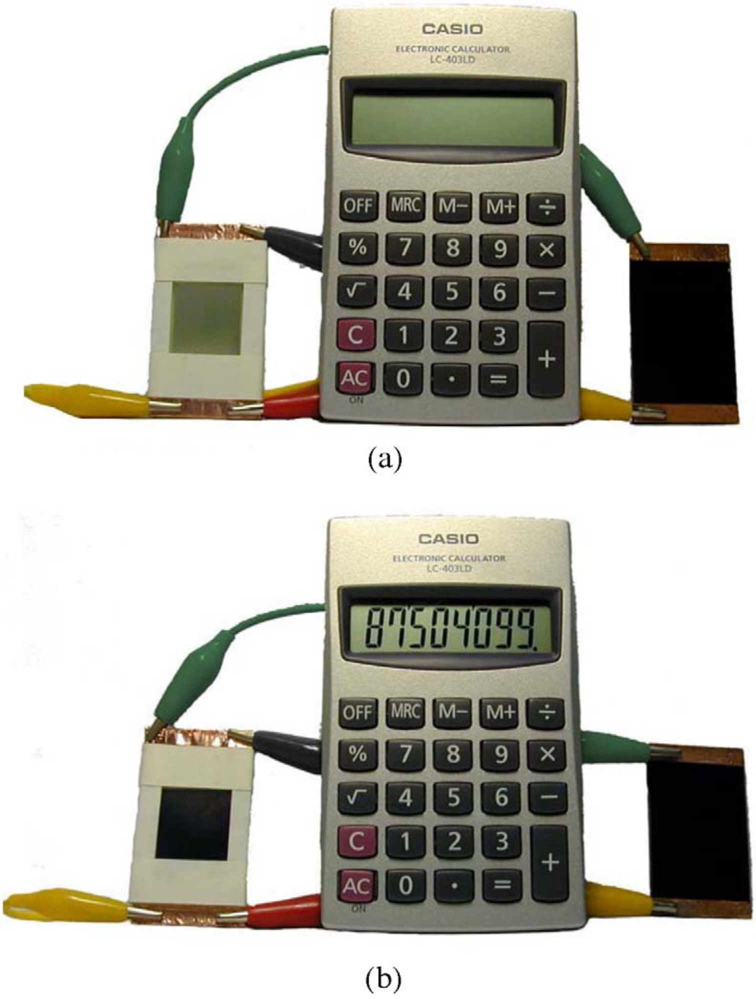

(a)

(b)

Fig. 3. Demonstration of an all-solar-driven electronic calculator based on the combinative PV–ECB power system: (a) before charging; (b) after charging.

above facts, a possible IWECB-based window is proposed. Such a window can be charged by a PV cell in the daytime so that it not only stores solar energy but also changes color to attenuate incident sunlight. Then the charged, colored window can be bleached to increase interior illumination and to drive low-power electronic devices after sunset by discharging. Thus, an IWECB can offer multiple energy-saving functions.

3.2. Influences of KCl doping on SPE properties

3.2.1. pH and pK values of the monomer solution as a function of (KCl)/(AMPS)

As shown in Fig. 1, the KCl-saturated PAMPS SPE can result in an IWECB with satisfactory charge/discharge behavior, whereas PAMPS can not. Thus, the role of potassium ions doped into the SPE needs to be determined. PAMPS is a well-known proton conductor [18,19]. Randin [18] reported that the ionic conductivity of PAMPS is a function of both the temperature and the water content inside the SPE. His findings are summarized below. For the temperature range of − 20 ~ 50 °C, the conduction of protons in PAMPS was observed to be faster at higher temperature. The water inside PAMPS was classified into the bound water and free water. The reported number of water molecules tightly bound per sulfonic group was around 6. It was reported that the ionic conductivity increases as the number of bound water increases. However, when the molar ratio of free water to the sulfonic group $(H_2O)/(SO_3^-)$ was greater than 6, the ionic conductivity stopped increasing. Since InHCF prefers K^+ [20–24] and WO_3 prefers H^+ [25–27] for their EC kinetics, doping K^+ in PAMPS to attain the dual ionic conduction of both H^+ and K^+ is necessary for an IWECB. Habib et al. [37] also adopted a similar electrolyte system, in which polyvinyl alcohol was doped with H_3PO_4 and KH_2PO_4 for a complementary PB-WO_3 ECD. Doping different amounts of KCl would first lead to different (KCl)/(AMPS) molar ratios in the monomer solution and then affects the $[K^+]/[H^+]$ concentration ratio. Fig. 4 gives the pH and p*K* values of the monomer solutions under different (KCl)/(AMPS) conditions before polymerization. Note that the values of pH are negative, whereas the values of p*K* are positive. Because the monomer solution has the same amount of AMPS, the pH value is almost invariant. On the other hand, the p*K* value decreases proportionally as the (KCl)/(AMPS) ratio increases. This indicates that the molar ratio (KCl)/(AMPS) can be viewed as a measure of $[K^+]/[H^+]$ and thus can serve as a measure of the K^+-doping level in the SPE.

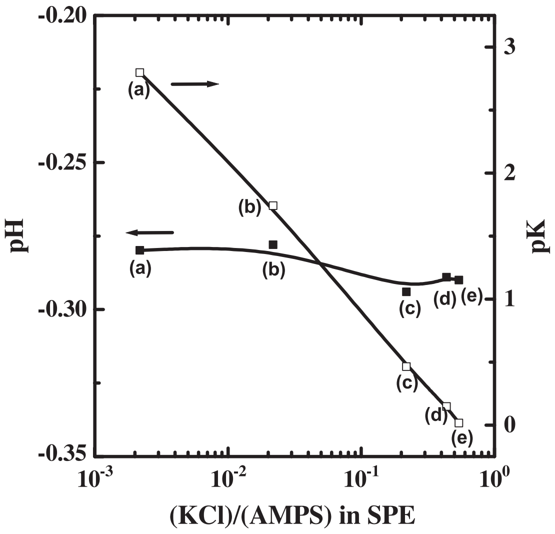

Fig. 4. The pH and p*K* values for the AMPS monomer solutions under different KCl-doping conditions before polymerization. (KCl)/(AMPS) denotes the molar ratio of KCl to AMPS.

3.2.2. Ionic conductivity and water content of the SPE as a function of (KCl)/(AMPS)

The ionic conductivity of the KCl-doped PAMPS SPE, measured at room temperature with impedance spectroscopy, is shown in Fig. 5. The ionic conductivity of the SPE exhibits a concave-up dependence on the KCl-doping level, and a minimum exists in the vicinity of (KCl)/(AMPS) = 0.44. The water content inside the SPE is also a function of (KCl)/(AMPS), as shown in Fig. 6. The water content in Fig. 6 follows a very similar tendency to that of the ionic conductivity in Fig. 5. It is found that the molar ratios of $(H_2O)/(SO_3^-)$ for all of the SPEs used in this work are larger than 6. Thus, free water [18] must exist inside the SPEs which were polymerized in air. Because K^+ migrates more slowly than H^+, a larger (KCl)/(AMPS) ratio implies a smaller fraction of H^+ in the SPE and thus gives a lower ionic conductivity. Both the ionic conductivity (Fig. 5) and water content (Fig. 6) decrease with an increase of

(KCl)/(AMPS) ratio up to 0.44 and then increase. The reason for the increase above 0.44 of (KCl)/(AMPS) is still unclear.

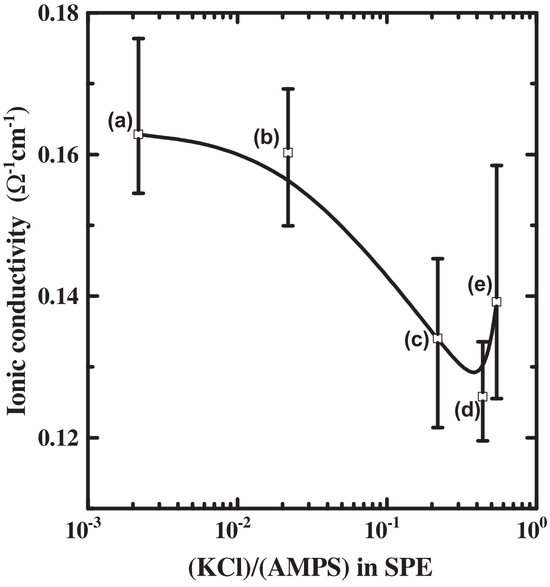

Fig. 5. Ionic conductivity of the KCl-doped PAMPS SPE as a function of (KCl)/(AMPS).

3.3. Influences of (KCl)/(AMPS) on the electrochemical behaviors of EC electrodes

In this subsection, the effects of (KCl)/(AMPS) on the electrochemical behaviors of EC electrodes are discussed. The CVs of the InHCF and WO_3 electrodes, in contact with the SPEs with different KCl-doping levels, are shown in Figs. 7 and 8, respectively. It can be seen in Fig. 7 that all of the CVs are similar in shape, but the formal potential shifts in the cathodic direction as (KCl)/(AMPS) decreases. This electrochemical behavior is consistent with that of the InHCF electrode immersed in an aqueous electrolyte [38]. Because insertion of K^+ into a PBA electrode follows the Nernst equation and the pK value in the monomer solution increases as (KCl)/(AMPS) decreases, the CV peak shifts with variations in the KCl-doping level. The peak current, which decreases as (KCl)/(AMPS) decreases, should be due to decay of the K^+ supply. Furthermore, decay of the cathodic peak current is larger than the anodic one. This means that the insertion of K^+ becomes more difficult than its extraction. When the formal potential is plotted vs. log [K^+], a slope of 0.064 V per decade [K^+] is obtained (not shown here). Such a slope is slightly higher than the theoretical value of

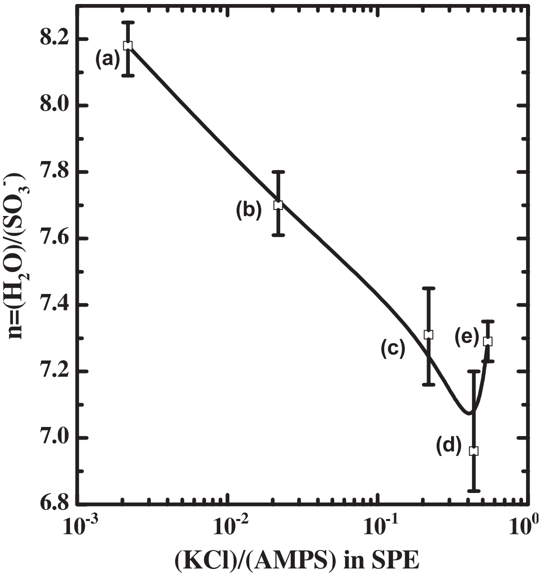

Fig. 6. Water content of the KCl-doped PAMPS SPE as a function of (KCl)/(AMPS). n represents the molar ratio of (H_2O) to (SO_3^-) in SPE.

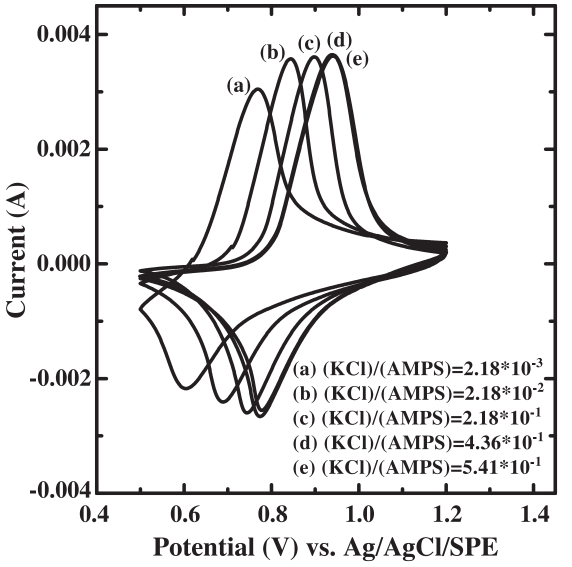

Fig. 7. Cyclic voltammograms for the InHCF electrodes in contact with different KCl-doped PAMPS SPEs. Scan rate is 5 mV/s, and electrode area is 2 × 2 cm^2.

0.059 V per decade [K^+]. The possible reasons are that [K^+] was measured in the monomer solution, and the realistic EC mechanism of InHCF is more complicated than that described in Eq. (1). As for the CVs of WO_3 shown in Fig. 8, there are no significant differences. The reasons are that the pH value in Fig. 4 is almost the same, and Eq. (2) is not affected by [K^+]. That is, the electrochemical behavior of WO_3 is less influenced by the (KCl)/(AMPS) ratio when the value of (AMPS) is fixed.

3.4. Influences of (KCl)/(AMPS) on the electrochemical performances of the IWECB

3.4.1. Effects on the discharge characteristics of the IWECB

The typical discharge curves for IWECBs of five different SPEs are shown in Fig. 9. The discharge time increases as (KCl)/(AMPS) increases. That is, the charge capacity of the IWECB increases when (KCl)/(AMPS) increases. This is because potassium ions are sufficiently supplied at a high KCl-doping level, as discussed in Section 3.3. In addition, when (KCl)/(AMPS) increases, the cell shows a higher mid-point discharge voltage and a more obvious flat discharge zone except for the case of (KCl)/(AMPS) = 0.00218. This can be explained by Fig. 7, in which reducing the amount of [K^+] leads InHCF's formal potential to shift in the cathodic direction. The exception at (KCl)/(AMPS) = 0.00218 is presumably due to incomplete discharge. Thus, the IWECB with the KCl-saturated PAMPS SPE shows the best performances from the viewpoints of charge capacity, mid-point discharge voltage, and flat discharge zone.

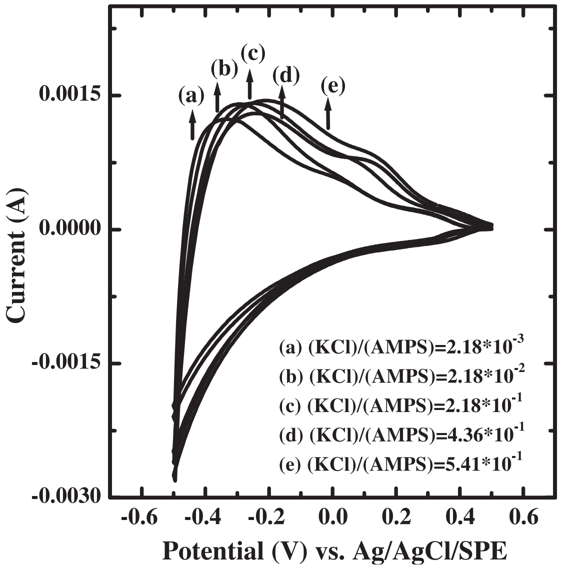

Fig. 8. Cyclic voltammograms for the WO_3 electrodes in contact with different KCl-doped PAMPS SPEs. Scan rate is 5 mV/s, and electrode area is 2×2 cm^2.

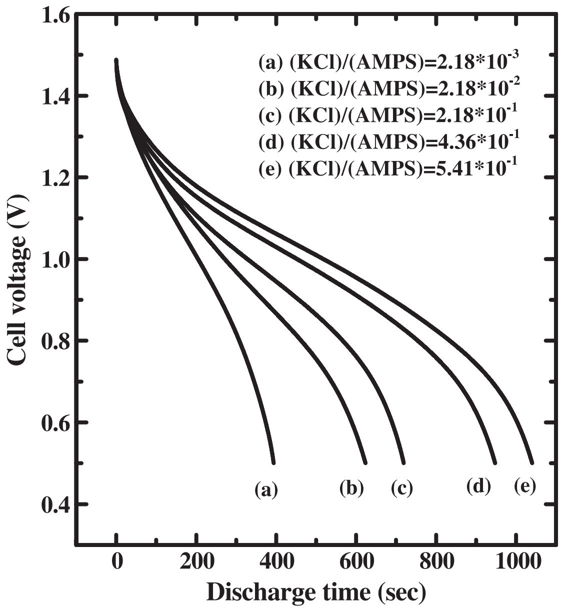

Fig. 9. Discharge curves for the IWECBs in combination with different KCl-doped PAMPS SPEs. Discharge rate is 0.025 mA/cm^2.

3.4.2. Effects on the cycle life of the IWECB

The cycling characteristics of the IWECBs, charged–discharged between 0.5 and 1.5 V 1000 times at a rate of 0.1 mA/cm^2, are compared in Fig. 10. The ratio of the discharge capacity of the *n*th cycle to that of 1st cycle, Q_n/Q_1, decreases as the cycle number increases. One possible reason is the molar ratio of $(H_2O)/(SO_3^-)$ inside the SPE is larger than 6, as shown in Fig. 6. Although the free water provides faster ionic conduction, it also causes degradation of WO_3 [39]. The other possible reason is the decomposition of InHCF at a high voltage. If these two degradations ever happen, the decomposition of InHCF is more crucial than the dissolution of WO_3 film because WO_3 has been reported to show electrochromic reactions more than 10^4 cycles even in an aqueous electro-

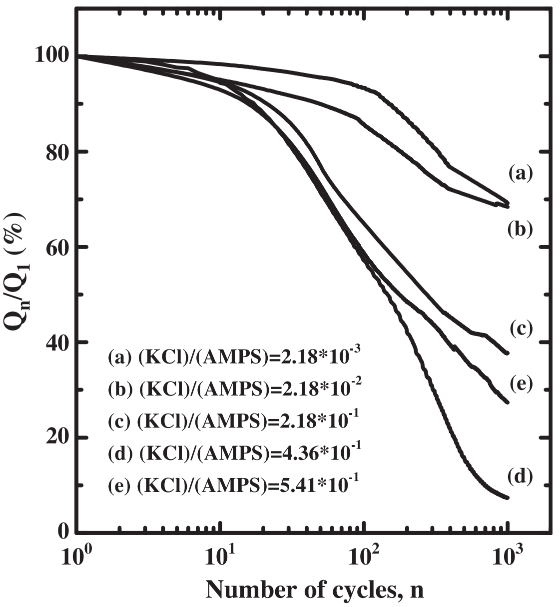

Fig. 10. Cycling stability for the IWECBs in combination with different KCl-doped PAMPS SPEs at a charge–discharge rate of 0.1 mA/cm^2. Q_n and Q_1 denote the discharge capacity of the cell at the nth and 1st cycle, respectively.

lyte such as a H_2SO_4. The most spectacular event in Fig. 10 is that the capacity decays more slowly at the lower KCl-doping level than at the higher level. Again, this can be explained by the incomplete discharge, as mentioned in Section 3.4.1. Although an IWECB using an SPE with a smaller (KCl)/(AMPS) ratio has a better cycle life, it has an inherently less-workable capacity and voltage. Thus, improving the cycle life of the IWECB using the KCl-saturated PAMPS is currently the most important issue. One possible strategy is to carefully select the applied voltage to avoid the decomposition of InHCF. The other is to properly control the water content inside the SPE to avoid the dissolution of WO_3. Some efforts are still needed to determine the optimal design of the IWECB using KCl-doped PAMPS SPE.

4. Conclusions

It is demonstrated in this work that the IWECB in combination with a KCl-doped PAMPS SPE can be charged/discharged reversibly between 0.5 and 1.5 V at a rate of 0.025 mA/cm^2. In addition, the IWECB shows vivid blue-to-colorless electrochromism when discharging, and the most obvious color change occurs at a cell voltage near the mid-way voltage of the charge–discharge curve (voltage vs. time). This means that the IWECB provides SOC visualization and can thus facilitate the use of such a secondary battery. By connecting to a PV cell, an IWECB can also act as a reservoir for solar energy collected from the PV cell and be darkened to serve as a solar-attenuating window during the daytime. When serving as a window, the energy stored in the IWECB can be discharged to drive low-power electronic devices, accompanied by bleaching the IWECB and increasing the interior illumination after sunset. As for the SPE, it was found in this work that the molar ratio of (KCl)/(AMPS) in the AMPS monomer solution considerably affects the properties of a KCl-doped PAMPS SPE. Generally, both the water content and ionic conductivity of the SPE decreases as (KCl)/(AMPS) increases (with KCl-saturated PAMPS being an exception). Logically, the modification of PAMPS (originally it is a polyelectrolyte for H^+) by doping with KCl can successfully accommodate the conduction of both K^+ and H^+. IWECBs with different KCl-doped PAMPS SPEs show very different performances. Among the SPEs with different KCl-doping levels, the KCl-saturated PAMPS SPE can result in a larger charge capacity, larger discharge voltage, and more obvious flat discharge zone. On the other hand, a poorer cycle life was also observed. To sum up, it is believed that KCl-doped PAMPS SPEs can promote other PB-based ECB and ECD systems.

Acknowledgements

The authors wish to thank Sinonar, Hsinchu, Taiwan, for providing the conductive F-doped SnO_2-coated glass substrates. This research was supported by the Program for Promoting Academic Excellence of Universities, sponsored by the Ministry of Education of the Republic of China, under grant no. Ex-91-E-FA09-5-4.

References

[1] P.M.S. Monk, R.J. Mortimer, D.R. Rosseinsky, Electrochromism: Fundamentals and Applications, VCH, Weinheim, Germany, 1995.

[2] B.W. Faughnan, R.S. Crandall, P.M. Heyman, RCA Rev. 36 (1975) 177.
[3] K. Itaya, K. Shibayama, H. Akahoshi, S. Toshima, J. Appl. Phys. 53 (1982) 804.
[4] F.G.K. Baucke, in: C.M. Lampert, C.G. Granqvist (Eds.), SPIE Institute Series, vol. IS4, 1990, pp. 518–538.
[5] R.D. Rauh, Electrochim. Acta 44 (1999) 3165.
[6] V.D. Neff, J. Electrochem. Soc. 132 (1985) 1382.
[7] K. Honda, J. Ochiai, H. Hayashi, J. Chem. Soc., Chem. Commun. (1986) 168.
[8] K. Honda, H. Hayashi, J. Electrochem. Soc. 134 (1987) 1330.
[9] M. Jayalakshmi, F. Scholz, J. Power Sources 87 (2000) 212.
[10] K. Kuwabara, J. Nunome, K. Sugiyama, J. Electrochem. Soc. 137 (1990) 2001.
[11] K. Kuwabara, J. Itoh, K. Sugiyama, J. Mater. Sci. 27 (1992) 5315.
[12] E.W. Grabner, S. Kalwellis-Mohn, J. Appl. Electrochem. 17 (1987) 653.
[13] M. Jayalakshmi, F. Scholz, J. Power Sources 91 (2000) 217.
[14] L.-C. Chen, Y.-H. Huang, K.-S. Tseng, K.-C. Ho, J. New Mater. Electrochem. Syst. 5 (2002) 203.
[15] L.-C. Chen, K.-S. Tseng, Y.-H. Huang, K.-C. Ho, J. New Mater. Electrochem. Syst. 5 (2002) 213.
[16] R.J. Mortimer, D.R. Rosseinsky, J. Electroanal. Chem. 151 (1983) 133.
[17] K. Itaya, I. Uchida, V.D. Neff, Acc. Chem. Res. 19 (1986) 162.
[18] J.P. Randin, J. Electrochem. Soc. 129 (1982) 1215.
[19] R.D. Giglia, U.S. Pat. 4,375,318, 1983.
[20] P.J. Kulesza, M. Faszynska, J. Electroanal. Chem. 252 (1988) 461.
[21] P.J. Kulesza, M. Faszynska, Electrochim. Acta 34 (1989) 1749.
[22] S. Dong, Z. Jin, Electrochim. Acta 34 (1989) 963.
[23] Z. Jin, S. Dong, Electrochim. Acta 35 (1990) 1057.
[24] K.C. Ho, J.C. Chen, J. Electrochem. Soc. 145 (1998) 2334.
[25] S.K. Deb, Appl. Opt., Suppl. 3 (1969) 193.
[26] R.S. Crandall, P.J. Wojtowicz, B.W. Faughnan, Solid State Commun. 18 (1976) 1409.
[27] C.G. Granqvist, Solar Energy Mater. Sol. Cells 60 (2000) 201.
[28] M.T. Nguyen, L.H. Dao, J. Electrochem. Soc. 136 (1989) 2131.
[29] B.P. Jelle, G. Hagen, Solar Energy Mater. Sol. Cells 58 (1999) 277.
[30] K.-C. Ho, T.G. Rukavina, C.B. Greenberg, J. Electrochem. Soc. 141 (1994) 2061.
[31] R. Spindler, U.S. Pat. 5,209,980, 1993.
[32] L.-C. Chen, Y.-H. Huang, K.-C. Ho, J. Solid State Electrochem. 7 (2002) 6.
[33] L.-C. Chen, K.-S. Tseng, K.-C. Ho, J. Solid State Electrochem. 7 (2002) 1.
[34] K. Yamanaka, H. Oakamoto, H. Kidou, T. Kudo, Jpn. J. Appl. Phys. 25 (1986) 1420.
[35] P.K. Shen, J. Syed-Bokhari, A.C.C. Tseung, J. Electrochem. Soc. 138 (1991) 2778.
[36] P.K. Shen, A.C.C. Tseung, J. Mater. Chem. 2 (1992) 1141.
[37] M.A. Habib, S.P. Maheswari, M.K. Carpenter, J. Appl. Electrochem. 21 (1991) 203.
[38] M.A. Malik, G. Horanyi, P.J. Kulesza, G. Inzelt, V. Kertesz, R. Schmidt, E. Czirok, J. Electroanal. Chem. 452 (1998) 57.
[39] T.C. Arnoldussen, J. Electrochem. Soc. 128 (1981) 117.